pH Tuning of DNA Translocation Time through Organically Functionalized Nanopores

Brett N. Anderson,[†] Murugappan Muthukumar,[‡] and Amit Meller*[,†]

[†]Department of Biomedical Engineering, Boston University, 44 Cummington St, Boston, Massachusetts 02215, United States and [‡]Polymer Science and Engineering Department, University of Massachusetts, 120 Governors Drive, Amherst, Massachusetts 01003, United States

ABSTRACT Controlling DNA translocation speed is critically important for nanopore sequencing as free electrophoretic threading is far too rapid to resolve individual bases. A number of promising strategies have been explored in recent years, largely driven by the demands of next-generation sequencing. Engineering DNA–nanopore interactions (known to dominate translocation dynamics) with organic coatings is an attractive method as it does not require sample modification, processive enzymes, or complicated and expensive fabrication steps. In this work, we show for the first time 4-fold tuning of unfolded, single-file translocation time through small, amine-functionalized solid-state nanopores by varying the solution pH *in situ*. Additionally, we develop a simple analytical model based on electrostatic interactions to explain this effect which will be a useful tool in designing future devices and experiments.

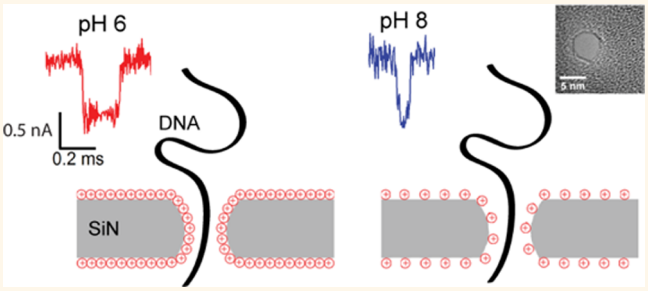

KEYWORDS: nanopore · DNA · translocation speed · single molecule · self-assembled monolayer · silane

Nanopore-based single-molecule sensors are being developed for variety of biotechnological applications, perhaps most notably next-generation sequencing.[1,2] Temporal resolution limitations are common to both biological and solid-state nanopore sensors as an analyte needs to reside within the pore long enough to make an accurate measurement over background noise. A number of advanced strategies have been developed to slow down or increase DNA translocation speed through nanopores *via* genetic engineering of protein pores,[3] active voltage control,[4,5] salt gradients,[6] transverse electric fields,[7] gate-modulation of wall surface charge,[8] electrolyte selection,[9] and coupling the analyte to processive enzymes such as molecular motors.[10,11] Here we present a simple alternative method which decouples translocation speed from modifications which might change the pore structure, require active voltage control (which also impacts capture rate and sensitivity), or add reliance on sensitive, sequence-dependent enzymatic processes.

Selective RNA and protein transport through nuclear pore complexes (NPC)[12] and DNA translocation through synthetic nanopores[13] are both exquisitely sensitive to interactions between the translocating biopolymers and the pore surface. In this work, inspired by the natural structure of biological nanopores, we investigate the effect of pH-sensitive organic layers internally coating nanopores. The formation of a polymeric cushion between the solid pore walls and the DNA[14] serves two functions: first, it prevents direct interactions or sticking of biopolymers to the pore walls; second, it lends itself to chemically induced surface charge modulation, which is shown here to modulate the translocation time. We note that this is the first report, to the authors' knowledge, of DNA translocation through small (<6 nm) chemically functionalized solid-state nanopores, which is necessary for technologies that require single-file translocation of unfolded DNA (such as nanopore sequencing).

RESULTS AND DISCUSSION

A schematic of our experiment is shown in Figure 1a. An electron beam from a

* Address correspondence to ameller@bu.edu.

Received for review November 6, 2012 and accepted December 22, 2012.

Published online December 22, 2012
10.1021/nn3051677

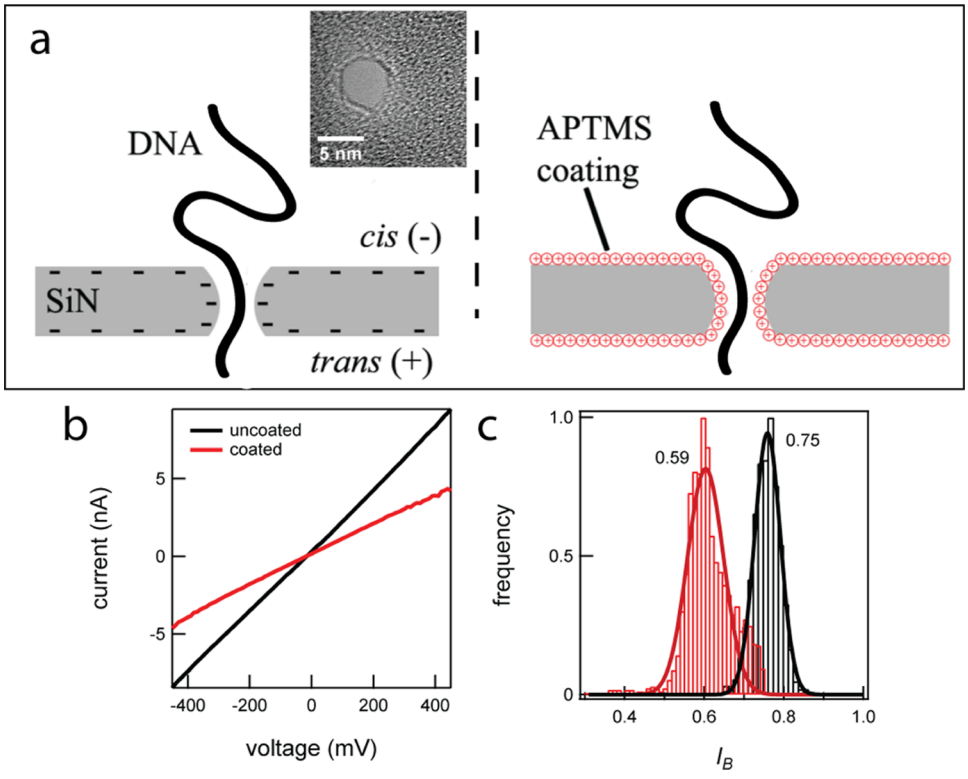

Figure 1. DNA translocation before and after APTMS coating. (a) Schematic of an uncoated and an APTMS-coated solid-state nanopore with DNA threading from *cis* to *trans*. Inset is a TEM image of a 5.2 nm nanopore before coating. (b) $I-V$ curves before (black) and after (red) coating a 5.7 nm pore in 1 M KCl pH 8.0. (c) Normalized blockade current (I_B) histograms measured using 4 kbp DNA under the same conditions as in panel b for uncoated and coated nanopores (black, n = 1525 and red, n = 1628).

transmission electron microscope (TEM) was used to drill nanopores with diameters of 5−6 nm (Figure 1a inset) in 45 nm silicon nitride (SiN) membranes as described previously.[15] After coating with 3-(aminopropyl)trimethoxysilane (APTMS), we can induce surface charge inversion when the pH is below the point of zero charge, rendering the surface slightly positive. Initial characterization of a typical 5.7 ± 0.1 nm nanopore, as measured by HR-TEM, was performed by measuring its current−voltage ($I-V$) curve before and after coating (Figure 1b, black and red traces, respectively). From the reduction in the linear pore conductance after coating we estimate an effective geometric reduction in the pore diameter Δd = 1.0 ± 0.2 nm by assuming that the nanopore is a perfect cylinder and that $\Delta d = d_O(1 - (G_C/G_O)^{1/2})$, where d_O is the diameter before coating as measured by electron microscopy, G_C is the conductance after coating, and G_O is the conductance before coating. This simple approximation corresponds well with a theoretical monolayer thickness of ~0.6 nm for APTMS and is consistent with previous work.[14] We note, however, that this estimation does not take into account the possibility of charge flow through the polymer layer and also only crudely approximates the solid-state nanopore as a perfect cylinder (when it is known to have a more complicated double-conical structure[15]), and it thus serves only as a confirmation that a stable layer is formed inside the pore.

We have previously reported that the normalized blockage of a pore I_B is dependent on pore size, d, as $I_B = i_b/i_o = 1 - (a/d)^2$, where i_b is the blocked-level current, i_o is the open-pore current, and a = 2.2 nm is the average dsDNA diameter, and is independent of the DNA length, N, as long as the DNA is shorter than approximately 1 kbp. For longer DNA molecules we observed a decrease in I_B as a function of N, which could be empirically fit to a 0.49 ± 0.10 power law.[13] The measurements of I_B before and after coating (using the same DNA molecules) can thus provide another indirect measurement of the effective pore size. The measured I_B before (0.75 ± 0.02, n = 1525) and after (0.59 ± 0.02, n = 1628) coating for a typical experiment using 4 kbp DNA (Figure 1c) is consistent with translocations through 6.6 ± 0.3 nm and 4.0 ± 0.2 nm uncoated pores, respectively.[13] The discrepancy between I_B and conductance estimations of pore diameter may be a result of direct interaction of DNA with the coated pore wall and a higher relative blockage of pore-surface associated current. Furthermore, DNA itself is a highly charged molecule and DNA-associated current may play a small role in changing the overall conductance of a nanopore during translocation.

To understand the effect of surface charge on DNA translocation dynamics, one has to consider two possible mechanisms: (i) electro-osmotic flow (EOF) of anions (in the case of positively charged surface) and

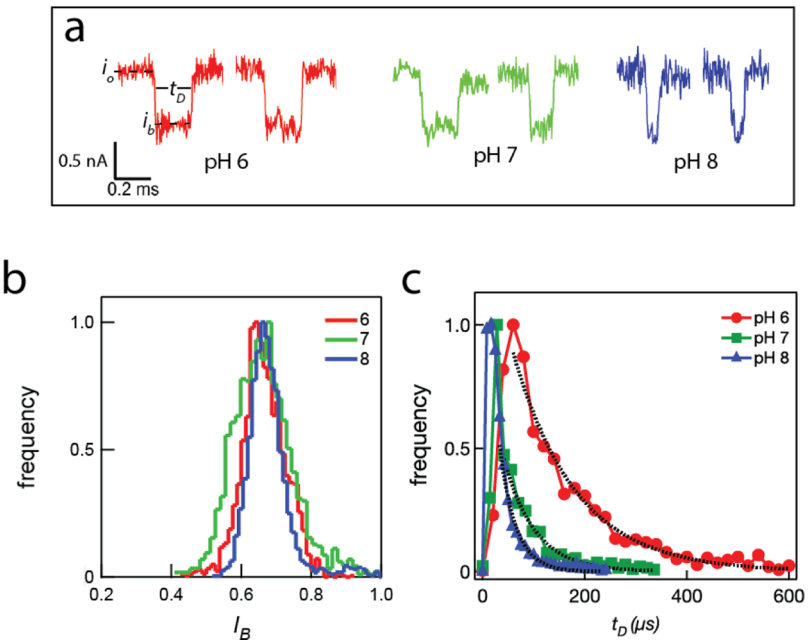

Figure 2. Translocation time through a coated pore can be sped up or slowed down by changing pH. (a) 1 kbp DNA translocating through a coated 5.2 nm pore at pH 6.0 (red), 7.0 (green), and 8.0 (blue) and characterized by open-pore current i_o, blocked-level current i_b, and dwell time t_D. (b) I_B histograms at pH 6.0, 7.0, and 8.0. (c) t_D histograms at pH 6.0, 7.0, and 8.0 with corresponding exponential time scales t_{pH6} = 118 μs, t_{pH7} = 46 μs, and t_{pH8} = 29 μs (n = 1000−3000 events analyzed for each pH in the same pore).

(ii) direct electrostatic nonspecific interactions of the negatively charged DNA with the pore walls. Changing the pH in our system provides a convenient way to affect both mechanisms as at lower pH the surface is more protonated resulting in a larger positive surface charge. Typical events of 1 kbp DNA translocating through a coated pore at pH 6.0, 7.0, and 8.0 are shown in Figure 2a with decreasing dwell times as pH increases. We note that the noise level in these events is larger than the typical noise we obtain using uncoated pores for reasons that are not currently known, though we speculate that changes to the surface chemistry and membrane capacitance may be responsible. When 1 kbp DNA was translocated through a coated 5.2 ± 0.1 nm pore at pH 6.0, 7.0, and 8.0, neither i_O (2.6 ± 0.1 nA) nor I_B (0.65 ± 0.01) were observed to change significantly with pH (Figure 2b). This observation is consistent with prior measurements using larger solid-state nanopores[16] as well as chemically coated pores[14] in that the relative bulk current flow becomes much larger than wall surface flow for weakly charged pores at high salt (>0.5 M KCl), and, as such, the I_B signal should be relatively insensitive to small changes in the surface charge with the pH at 1 M KCl. Dwell times, however, shifted substantially as can be seen in Figure 2c. We characterized the typical translocation time by exponential-tail fits to the dwell-time histograms yielding 118 ± 12 μs, 46 ± 8 μs, and 29 ± 4 μs at pH 6.0, 7.0, and 8.0, respectively. Given that I_B is very sensitive to the structure of dsDNA[17] and we observe no large shift with pH, we can assume that the shift in dwell times is not due to small changes in DNA structure. Taken together it appears that the dominating effect in our system is DNA−wall interaction, which becomes more prominent at lower pH (more positive surfaces), rather than the EOF which is expected to yield faster translocation time at low pH, contrary to our data.

To investigate whether pH tuning has a dependence on length, two additional DNA lengths were translocated at pH 8.0 and 6.0. Figure 3 shows the translocation distribution times of 1 kbp, 4 kbp, and 10 kbp dsDNA, measured either at pH 8.0 (blue circles) or pH 6.0 (red circles) using a 5.6 ± 0.1 nm pore. Consistent with the results presented in Figure 2, we observe a similar increase in the typical translocation time at the lower pH value. Within this range of DNA lengths, the pH-tuning effect was observed for all samples and does not appear to be strongly dependent on the molecule's length or composition. Table 1 summarizes the characteristic translocation time scales for the three DNA lengths (obtained by exponential fits to the tail of the t_D distributions) and the amount of translocation enhancement for the three DNA molecules. In comparison we show a control measurement using an uncoated nanopore and 1 kbp DNA with no translocation time modulation with pH. Our results indicate that within this pH range all DNA lengths exhibit similar translocation enhancement. We also tested the effect of the initial nanopore diameter on the translocation enhancement. A 5.2 nm pore with 1 kbp DNA had a 4-fold enhancement in translocation time when

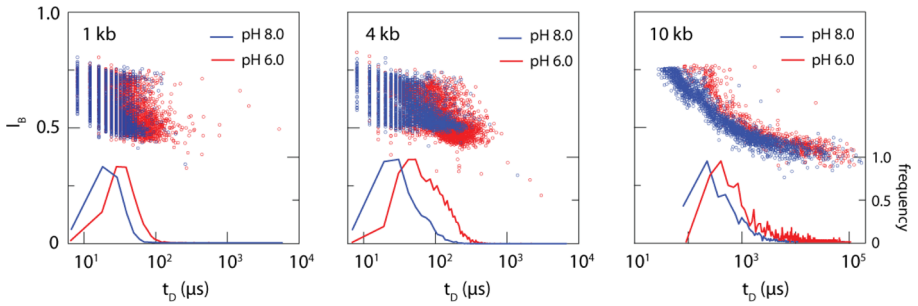

Figure 3. Tuning translocation time for three lengths of DNA (1, 4, and 10 kbp) in 5.6 ± 0.1 nm coated pores at pH 6.0 (red) and 8.0 (blue). Main figure displays I_B *vs* t_D event diagrams (>1000 events per experiment) and lower insets show normalized t_D histograms.

TABLE 1. DNA Translocation Time Scales Extracted from Exponential-Tail Fits to the t_D Histograms

	t (μs)			
	uncoated 1 kb	coated 1 kb	4 kb	10 kb
pH 6.0	11 ± 2	25 ± 2	84 ± 6	236 ± 20
pH 8.0	12 ± 3	12 ± 1	47 ± 3	95 ± 8
t/t_{pH8}	0.9 ± 0.3	2.1 ± 0.2	1.8 ± 0.2	2.5 ± 0.3

shifting between pH 8.0 and 6.0 compared to a 5.6 nm pore with only a 2-fold effect using the same DNA length (Figure 4 solid squares and circles, respectively). As a reference, no enhancement in translocation time was observed using the 1 kbp DNA and an uncoated 5.4 nm pore (open circles). In summary, for all DNA lengths and coated pore sizes, the translocation time increased as the solution became more acidic with smaller pores exhibiting a more pronounced effect.

Presumably, below pH 6.0 or above pH 8.0, the modulation of DNA translocation time through both coated and uncoated SiN nanopores would be stronger as the surface became more positively or negatively charged (the point of zero charge of bare SiN is near pH 4.1[18]); however, experiments attempted at pH lower than 6.0 or higher than 8.0 were unfeasible because the open-pore currents exhibited large fluctuations and pores tended to become blocked prematurely, preventing us from acquiring enough events to analyze. We hypothesize that the APTMS-coated pore becomes more strongly charged and DNA begins to stick and block the pore at low pH values and that the pore becomes negative at higher pH, repelling DNA and lowering capture rate, consistent with a point of zero charge for APTMS near pH 6−7.[19]

While measuring the surface charge density directly within a nanopore is difficult, colloid analogues of our system are experimentally accessible. 3-Aminopropyl-functionalized 100-nm silica nanoparticles (Sigma) were used to measure ζ potential in 1 M KCl at pH 6.0, 7.0, and 8.0 (Supporting Information, Figure S3), which we then used to calculate surface charge σ (see Supporting Information for details). We found the surface to be weakly positive within this range (σ decreased from 45.7 mC/m^2 at pH 6.0 to 11.4 mC/m^2

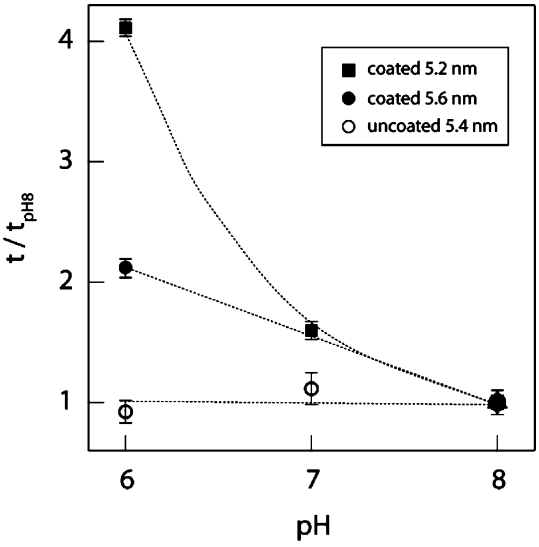

Figure 4. Relative dwell times *vs* pH for 1 kbp DNA and different pore diameters. The dwell times are normalized to their corresponding value at pH 8.0 to allow comparison under different conditions. Squares represent a coated 5.2 nm pore, solid circles a coated 5.6 nm pore, and open circles an uncoated 5.4 nm pore. Lines serve as guides to the eye.

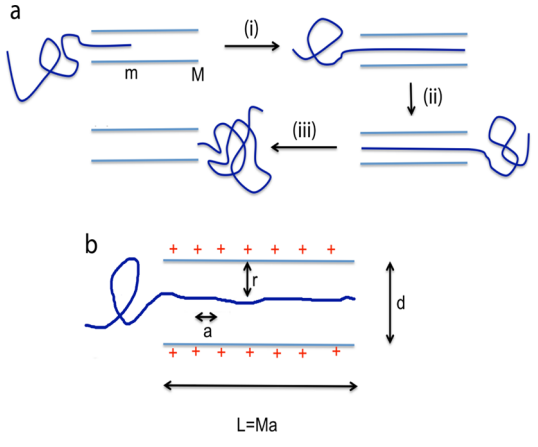

Figure 5. (a) Stages of the DNA translocation process. (b) Simple cylindrical model of DNA−nanopore electrostatic interactions.

at pH 8.0). It is likely that this approximates an upper limit for the surface charge relative to a nanopore system given that it is possible to form more dense monolayers on convex surfaces like spherical particles than within highly concave nanopores.

Analytical Model. To explain the strong dwell-time dependence on pH, we developed a simple analytical model for our system. The translocation of DNA through an oppositely charged nanopore consists of three stages: (i) filling the nanopore, (ii) transfer of monomers from the donor to the receiver compartment, and (iii) peeling off of the polymer from the pore, as illustrated in Figure 5. We follow the theory of refs 20 and 21 and derive the free energy landscape for the translocation process by considering the electrostatic interaction energy between the pore and the polymer and the drift force from the externally imposed electric field. First, the electrostatic interaction energy of a partially filled nanopore can be obtained as follows. Let the diameter and the length of a uniformly surface-charged cylindrical nanopore be d and $L \equiv Ma$, respectively, where a is the distance between two base pairs along the helix axis of DNA (Figure 5b). Let σ be the surface charge density on the pore. Assuming that the Debye−Hückel potential is valid, the pore-polymer interaction energy for a chain that has advanced a distance of ma inside the pore is given by

$$\frac{U_{el}(m)}{k_BT} = -q(\sigma a^2)\frac{\ell_B}{a}\frac{\pi d}{a}\int_0^m dm' \int_0^M dm'' \frac{\exp(-\kappa a\sqrt{(m'-m'')^2+(r/a)^2})}{\sqrt{(m'-m'')^2+(r/a)^2}} \quad (1)$$

Here, κ is the inverse Debye length for the electrolyte solution, r is the perpendicular distance between the mth charged unit of the polymer and the surface, q is the effective charge per monomer of the translocating polymer inside the pore, k_B is the Boltzmann constant, and $\ell_B = \frac{e^2}{4\pi\varepsilon_0\varepsilon_R k_B T}$ is the Bjerrum length, where e is the elementary charge, ε_0 is the permittivity of vacuum, and ε_R is the relative permittivity. Although $U_{el}(m)$ can be readily computed for a given set of values of σ, ℓ_B, d, and r, we lump these together in terms of one parameter ε and rewrite

$$\frac{U_{el}(m)}{k_BT} = -\varepsilon m \quad (2)$$

Numerical calculations of eq 1 for representative values of the parameters pertinent to our experimental conditions support the proportionality of U_{el} to m. The parameter ε is positive for oppositely charged pores and increases with the surface charge density. As the pH inside the pore is lowered, σ increases, and as a result ε increases.

The gain in free energy due to the externally imposed electric field for the partially filled nanopore is given by

$$\frac{U_{ext}(m)}{k_BT} = \frac{qe\Delta V m^2}{2Mk_BT} \quad (3)$$

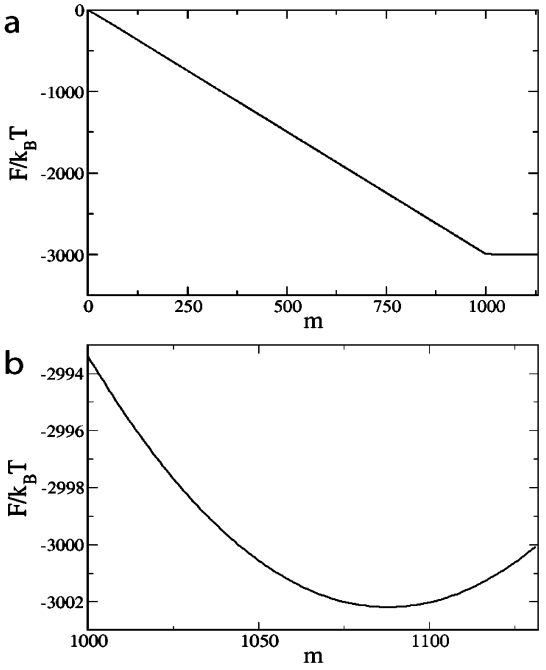

Figure 6. (a) Free-energy landscape during DNA translocation. (b) Electrostatic barrier as a function of the number of bases inside the pore.

where the voltage drop ΔV across the pore is assumed to be linear and e is the unit electronic charge.

The free energy of the polymer as it is threading through the pore is obtained by combining the above two equations and recognizing that when x charged monomers are transferred from the donor to the receiver compartment, there is a net electrochemical potential gain of $q_{trans}e\Delta Vx/k_BT$ in units of k_BT. The value of the effective charge q_{trans} for the monomer in the receiver compartment can in principle be quite different from the value inside the pore due to different levels of counterion adsorption. On the basis of the Manning argument, q_{trans} is about 0.25. Combining the above results, the free energy landscape for the translocation process is given by

$$\frac{F(m)}{k_BT} = \begin{cases} -\varepsilon m - \frac{qv}{2M}m^2, & 0 \le m \le M \\ -\varepsilon M - v(m-M) - \frac{qv}{2}M, & M \le m \le N \\ -\varepsilon(N+M-m) - v(m-M) - \frac{qv}{2M}(M^2-(m-N)^2), & N \le m \le N+M \end{cases} \quad (4)$$

where $v \equiv q_{trans}\, e\Delta V/k_BT$. The three expressions on the right-hand side correspond to the stages (i), (ii), and (iii), respectively, in Figure 5a. A typical landscape is given in Figure 6a, where $v = 3.0$ (corresponding to $\Delta V = 300$ mV and $q_{trans} = 0.25$), $M = 132$ (corresponding to the pore length of 45 nm, with $a = 0.34$ nm), $q = 0.1$, $\varepsilon = 2.8$, and $N = 1000$ (corresponding to 1 kbp DNA). For such strong electric fields in our experiments, the contribution from conformational entropy of the tail-like conformations of the polymer outside the pore is negligible and thus is

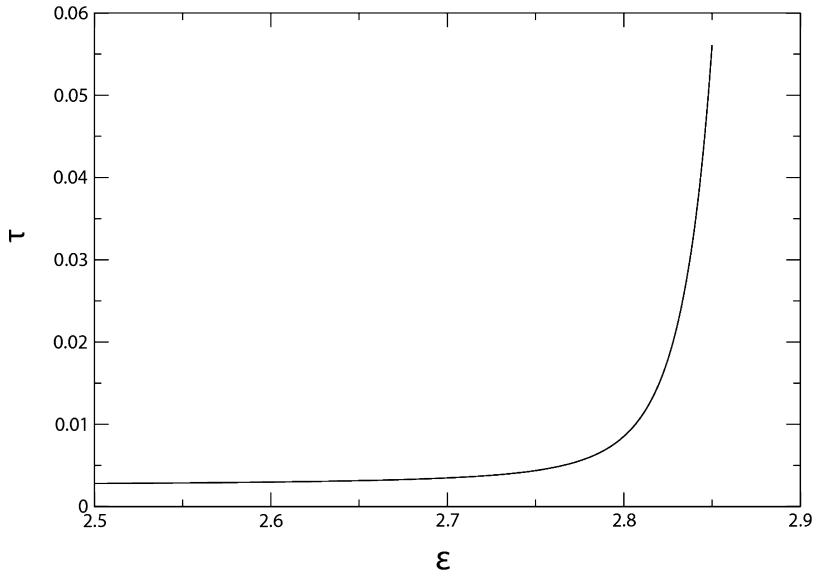

Figure 7. Translocation time τ (arbitrary units) as a function of ε.

ignored in the above equation. The role of the attractive electrostatic interaction between the pore and the polymer is manifest as an electrostatic barrier (Figure 6b) during the stage of ejection of the polymer from the pore. For the above set of parameters, this barrier is about $2k_BT$.

As evident from our experimental observations, the polymer very rarely retracts back into the donor compartment after some monomers are threaded through the pore. In view of this, we use the reflecting boundary condition in the calculation of the mean translocation time τ as described in ref 21,

$$\tau = \frac{1}{k}\int_0^{N+M} dm \int_0^{m} dm' \exp\left[-\frac{F(m)}{k_BT} - \frac{F(m')}{k_BT}\right] \quad (5)$$

where k is a phenomenological unknown parameter denoting the local friction of a monomer. The mean translocation time for the above choice of the parameters is given in Figure 7 as a function of ε, with τ in arbitrary units ($k = 10^6$). It is evident that τ depends weakly for small values of ε and after a threshold value of ε, τ increases significantly. In the latter regime, even a small change in the surface charge density can lead to substantial slowing down of the polymer.

CONCLUSION

With a variety of positive and negative organosilanes available, pores of a given geometry can be optimized for a range of sensing applications. Future work will explore translocation through noncharged and negatively charged coated pores to better characterize the relative importance of hydrophobicity, charge, and EOF on translocation dynamics. Theoretically, a similar but positively charged organosilane should have opposing contributions from EOF but similar hydrophobicity and therefore may prevent sticking of DNA while also allowing for tuning of translocation time *in situ* as demonstrated here. Furthermore, using nonionizable silanes with polar and nonpolar head groups will allow us to explore the importance of substrate hydrophobicity independent of surface charge and pH-induced conformational changes in the DNA which are certainly significant at extreme pH but may have more subtle effects near 7.

In summary, we demonstrated that by modifying the surface properties of solid-state nanopores, interactions between analyte and pore surface, and thus translocation dynamics, can be independently tuned. Our simple analytical model indicates, at least qualitatively, that small changes in surface charge can account for the large shifts we observe in dwell time, which enables us to adjust the translocation time without affecting other experimental conditions such as voltage or ionic strength (required for high S/B detection of the ionic current).

METHODS

The nanopores used in this study were fabricated in 45-nm thick free-standing SiN membranes with a focused electron beam[15] and chemically functionalized with monolayers of APTMS (Sigma) as previously described.[14] Briefly, the chips were heated to 120 °C in piranha solution (3:1 sulfuric acid to 35% wt hydrogen peroxide in water) for 15 min, rinsed thoroughly with Milli-Q water, immersed in 1% APTMS/methanol solution for 1 h, rinsed in methanol and water, then baked at 100 °C for 45 min, rewet in methanol, then transferred to 1 M KCl 10 mM phosphate-HCl at pH 6.0, 7.0, or 8.0.

DNA translocations through the APTMS-coated pores were performed by adding 250 ng of 1, 4, or 10 kbp DNA (Fisher, NoLimits) to the 50 μL *cis* reservoir for a final concentration of 1−8 nM and 300 mV applied (with the anode in the *trans* chamber and the cathode in the *cis*) with an Axopatch 200B patch-clamp amplifier from Molecular Devices. The electrical

signal was filtered using a four-pole Bessel low-pass at 100 kHz and sampled at 250 kHz/16 bits using a DAQ card (NI-6534) and custom LabVIEW software, used to detect/save events and control the voltage applied across the pore. In a typical experiment, 1000−3000 events were analyzed with custom software in Igor Pro (WaveMetrics) to generate dwell-time and current amplitude histograms. A single-exponential fit to the tail of the dwell-time distribution was used to characterize the event time scales for 1 kbp and 4 kbp and a double-exponential fit was used for 10 kbp (with corresponding time scales t and t' as explained in ref 12) with a $\chi^2 < 1.4$.

Conflict of Interest: The authors declare no competing financial interest.

Acknowledgment. Acknowledgement is made to the National Institutes of Health (Grants No. R01-HG005871 and R01-HG002776), National Science Foundation (Grant No. DMR 1105362), AFOSR (Grant No. FA9550-10-1-0159), and the Materials Research Science and Engineering Center at the University of Massachusetts, Amherst. We thank M. Wanunu for his assistance and advice in the early stages of this work.

Supporting Information Available: t_D histograms of control experiments, zeta potential measurements, and derivation of surface charge from zeta potential. This material is available free of charge *via* the Internet at http://pubs.acs.org.

REFERENCES AND NOTES

1. Venkatesan, B. M.; Bashir, R. Nanopore Sensors for Nucleic Acid Analysis. *Nat. Nanotechnol.* **2011**, *6*, 615–624.
2. Branton, D.; Deamer, D. W.; Marziali, A.; Bayley, H.; Benner, S. A.; Butler, T.; Di Ventra, M.; Garaj, S.; Hibbs, A.; Huang, X.; *et al.* The Potential and Challenges of Nanopore Sequencing. *Nat. Biotechnol.* **2008**, *26*, 1146–1153.
3. Rincon-Restrepo, M.; Mikhailova, E.; Bayley, H.; Maglia, G. Controlled Translocation of Individual DNA Molecules through Protein Nanopores with Engineered Molecular Brakes. *Nano Lett.* **2011**, *11*, 746–750.
4. Meller, A.; Nivon, L.; Branton, D. Voltage-Driven DNA Translocations through a Nanopore. *Phys. Rev. Lett.* **2001**, *86*, 3435–3438.
5. Bates, M.; Burns, M.; Meller, A. Dynamics of DNA Molecules in a Membrane Channel Probed by Active Control Techniques. *Biophys. J.* **2003**, *84*, 2366–2372.
6. Wanunu, M.; Morrison, W.; Rabin, Y.; Grosberg, A. Y.; Meller, A. Electrostatic Focusing of Unlabelled DNA into Nanoscale Pores Using a Salt Gradient. *Nat. Nanotechnol.* **2010**, *5*, 160–165.
7. Tsutsui, M.; He, Y.; Furuhashi, M.; Rahong, S.; Taniguchi, M.; Kawai, T. Transverse Electric Field Dragging of DNA in a Nanochannel. *Sci. Rep.* **2012**, *2*, 394.
8. He, Y.; Tsutsui, M.; Fan, C.; Taniguchi, M.; Kawai, T. Controlling DNA Translocation through Gate Modulation of Nanopore Wall Surface Charges. *ACS Nano* **2011**, *5*, 5509–5518.
9. Kowalczyk, S. W.; Wells, D. B.; Aksimentiev, A.; Dekker, C. Slowing Down DNA Translocation through a Nanopore in Lithium Chloride. *Nano Lett.* **2012**, *12*, 1038–1044.
10. Cherf, G. M.; Lieberman, K. R.; Rashid, H.; Lam, C. E.; Karplus, K.; Akeson, M. Automated Forward and Reverse Ratcheting of DNA in a Nanopore at 5-A precision. *Nat. Biotechnol.* **2012**, *30*, 344–348.
11. Manrao, E. A.; Derrington, I. M.; Laszlo, A. H.; Langford, K. W.; Hopper, M. K.; Gillgren, N.; Pavlenok, M.; Niederweis, M.; Gundlach, J. H. Reading DNA at Single-Nucleotide Resolution with a Mutant MspA Nanopore and phi29 DNA Polymerase. *Nat. Biotechnol.* **2012**, *30*, 349–353.
12. Hoelz, A.; Debler, E. W.; Blobel, G. The Structure of the Nuclear Pore Complex. *Annu. Rev. Biochem.* **2011**, *80*, 613–643.
13. Wanunu, M.; Sutin, J.; McNally, B.; Chow, A.; Meller, A. DNA Translocation Governed by Interactions with Solid-State Nanopores. *Biophys. J.* **2008**, *95*, 4716–4725.
14. Wanunu, M.; Meller, A. Chemically Modified Solid-State Nanopores. *Nano Lett.* **2007**, *7*, 1580–1585.
15. Kim, M. J.; Wanunu, M.; Bell, D. C.; Meller, A. Rapid Fabrication of Uniformly Sized Nanopores and Nanopore Arrays for Parallel DNA Analysis. *Adv. Mater.* **2006**, *18*, 3149–3153.
16. Smeets, R. M.; Keyser, U. F.; Krapf, D.; Wu, M. Y.; Dekker, N. H.; Dekker, C. Salt Dependence of Ion Transport and DNA Translocation through Solid-State Nanopores. *Nano Lett.* **2006**, *6*, 89–95.
17. Singer, A.; Kuhn, H.; Frank-Kamenetskii, M.; Meller, A. Detection of Urea-Induced Internal Denaturation of dsDNA Using Solid-State Nanopores. *J. Phys.: Condens. Matter* **2010**, *22*, 454111.
18. Hoogerheide, D. P.; Garaj, S.; Golovchenko, J. A. Probing Surface Charge Fluctuations with Solid-State Nanopores. *Phys. Rev. Lett.* **2009**, *102*, 256804.
19. Metwalli, E.; Haines, D.; Becker, O.; Conzone, S.; Pantano, C. G. Surface Characterizations of Mono-, Di-, and Triaminosilane Treated Glass Substrates. *J. Colloid Interface Sci.* **2006**, *298*, 825–831.
20. Muthukumar, M. *Polymer Translocation*; Taylor and Francis: Boca Raton, 2011; pp xvi, 354.
21. Muthukumar, M. Polymer Escape through a Nanopore. *J. Chem. Phys.* **2003**, *118*, 5174–5184.